Lasers in Manufacturing Conference 2021

Glass to copper direct welding with a rough surface by femtosecond laser pulse bursts

Qingfeng Li[a,*], Gabor Matthäus[a], Stefan Nolte[a,b]

[a]*Institute of Applied Physics, Abbe Center of Photonics, Friedrich Schiller University Jena, Albert-Einstein-Straße 15, 07745 Jena, Germany*
[b]*Fraunhofer Institute for Applied Optics and Precision Engineering IOF, Center of Excellence in Photonics, Albert-Einstein-Straße 7, 07745 Jena, Germany*

Abstract

We report on the welding of the borosilicate optical glass to a surface-unpolished copper substrate (Ra of 0.27 µm and Rz of 1.89 µm) using bursts of femtosecond laser pulses. By investigating the effects of the pulse energy and the focal position on the weldability, we confirmed that the glass melting and having the molten glasses fill the gap are the prerequisite conditions for the successful glass-to-metal welding. The factors that lead to those conditions are discussed. Under the optimal conditions, without the assistance of any clamping system, our welded samples kept a breaking resistance of up to 10.9 MPa.

Keywords: femtosecond laser; micro-welding; ultrafast processing; glass-metal-bonding;

1. Introduction

With the advantages such as high space-selectivity, low thermal residual effects and micron-dimension processing, the ultra-short pulsed (USP) laser welding has become a popular alternative technique for the brittle materials (e.g. glass (Richter *et al.*, 2013), ceramic (Penilla *et al.*, 2019)) welding, and dissimilar materials (e.g. glass-metal (Carter *et al.*, 2014), glass-silicon (Miyamoto *et al.*, 2015), glass-SiC (Zhang *et al.*, 2017), and silicon-metal (Chambonneau *et al.*, 2021)) welding. However, among all those proof-of-principle demonstration, a direct contact (so-called optical contact) is required. To overcome this prerequisite and adapt the local laser welding for mass production and industrial application, USP laser welding with a gap-

* Corresponding author. Tel.: +49(0)3641 | 9-47897; fax: +49 3641 947802.
E-mail address: qingfeng.li@uni-jena.de.

preserved condition has been insensitively investigated (Chen *et al.*, 2015, 2019; Cvecek *et al.*, 2015; Richter *et al.*, 2015; Zhang and Cheng, 2015; Carter *et al.*, 2017).

For the glass-to-glass configuration, the gap bridging mechanisms are confirmed by two independent experimental results published in the year of 2015 (Chen *et al.*, 2015; Richter *et al.*, 2015). The gap bridging process and can be summarized as: (i) thermal accumulation effect creates sufficient heat affected zone (HAZ), (ii) laser focus position is close enough to the interface so that the molten material within the HAZ can reach the surface, and (iii) the ejection or mixing of the molten material fill and form continuous structure within the gap. The maximum-bridged gap was about 3 µm.

For the glass-to-metal configuration, the gap bridging mechanisms are so far not clear. Contradictory results have been reported from different groups. In 2015, Zhang (Zhang and Cheng, 2015) reported femtosecond laser welding of alumina-silicate to copper, steel and aluminum welding with a pulse duration of 160 fs and a repetition rate of 1~kHz. The samples are mirror-polished, however without clamping. Under this repetition rate, thermal accumulations and the HAZ in glass are negligible; therefore, they have attributed the adhesive to the metal particles produced by laser ablation. They also claimed that the maximum bridgeable gap size depends on the stacking height of the ablated particles. Glass-to-metal welding under high repetition rate has also been reported (Carter *et al.*, 2017; Matsuyoshi *et al.*, 2018). In 2018 (Matsuyoshi *et al.*, 2018), laser welding of soda-lime glass to an unpolished copper without clamping was reported. In this experiment a laser with 550 fs pulse duration and 1~MHz repetition rate was used. Even though the thermal accumulation in glass is very likely took place under this repetition rate, in this paper the authors still attributed the adhesive to the ablation-induced metal particles. In (Carter *et al.*, 2017), with champing, SiO_2 and BK7 are welded to aluminum alloy with 5.9 ps laser at 400 kHz. With the help of a full range of electron microscopy methods (Ciuca *et al.*, 2016), they discovered that the metal melt volume is much smaller than the glass melt. Contradictory to the first interpretation, they believe that the glass melting and having the molten glass fill the gap is instrumental in metal-glass welding.

In this paper, we are aiming to weld glass onto an unpolished copper surface without any clamping. However, the aforementioned contradictory interpretations hindered our way of getting the optimized welding condition. Therefore, first of all, we have to find out which interpretation is closer to the nature of having successful welding and to discover the prerequisites conditions of having successful glass-to-metal welding. Afterwards, based on the prerequisites, we investigated the processing windows for achieving such conditions and used the borosilicate optical glass and a surface-unpolished copper substrate (Ra of 0.27 µm and Rz of 1.89 µm) to demonstrate the welding.

2. Methodology

2.1. Glass-to-metal welding setups

For the glass-to-metal USP laser welding, we used a prototype Trumpf TruMicro 2030 Femto Edition laser with a wavelength of 1030 nm, a pulse duration of 300 fs, a repetition rate varied from 250 kHz to 2 MHz, and a pulse energy of up to 20 µJ. This prototype laser can also work in the pulses bursts operation modes. The temporal distance between the individual pulses within a burst is 20 ns, and the maximum number of pulses per burst is 8. The complete experimental setup is sketched in Fig 1. The applied pulse energy can be adjusted by a half-wave plate (HWP) and a polarized beam splitter. The output laser beam, with a diameter of 5 mm, is reduced by a Galilean type of telescope to fulfil the dimension of the spatial light modulator (SLM) arrays. The shaped beam is then relayed to fully illuminate the back aperture of the microscope objective lens (MO) through two relay lenses. This lens (Mitutoyo, M Plan Apo NIR, 10×) is mounted on a stage allowing its displacement along the optical axis z and place the focus at the desired position for the processing. The glass and metal can be moved together in the xy plane perpendicular to the optical axis z thanks to a positioning system (Aerotech, ALS 130). In this paper, we used the Gaussian beam for the processing.

In our experiments, we can perform three-dimensional *in-situ* monitoring of the welding process by means of two customized microscopy diagnostics. The first one is a reflective microscope that is utilized for determining the relative position of the focus with the respect to the sample interface by performing surface damage scans at energies near the breakdown threshold. The second one is a transmission microscope relying on white light illumination. The light passes through the sample along x axis, and images of the welding seams in the yz plane are recorded by another objective lens (Mitutoyo, M Plan Apo, 10×) associate with its corresponding tube lens and camera.

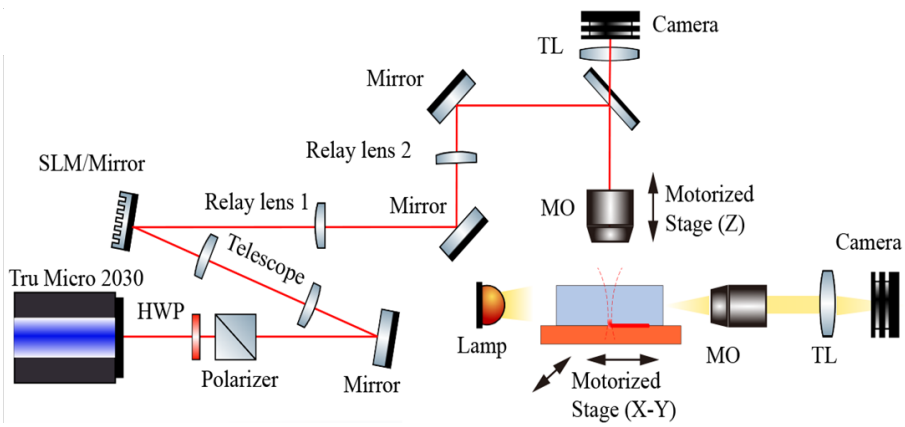

Fig. 1. Experimental setup for the glass-to-metal laser welding process. The pulses energy can be adjusted by the half-wave plate (HWP) and polarizer pair. A telescope is used to reduce the output beam diameter. A spatial light modulator (SLM) is used to generate desired beam shape. The shaped beam is then relayed using two relay lenses to fully illuminate the back aperture of the microscope objective lens (MO) that is used for processing. Through the same MO, a reflective microscope that used for controlling the focus position on the sample is setup thanks to the dichroic-mirror (DM), a tube lens (TL) and a camera. Additionally, through the horizontal lamp illumination a transverse microscope is setup to monitor the formation of the welding seams.

To achieve comparable results with what have been reported by other groups, the copper samples (99.99% pure) used in this paper were sourced by Goodfellow in half-hard temper condition without further polishing. The arithmetic average value of the surface roughness (Ra) is measured as 272 nm. Given that the surface has only finished with grinding, periodic serrated traces are left on the copper surface. The average value of the maximum peak to valley height (Rz) over the assessment length (12.9 mm) is measured as 1.89 µm. The glass samples used in this paper are 5 mm×5 mm×1 mm borosilicate glass (Schott Borofloat33) with λ/4 flatness. During the welding processing the glass plate was naturally stacked upon the copper without clamping.

2.2. Temperature evaluation

Even though a two temperature model is required to have precise description of the ultrashort pulse laser absorption (Kanavin *et al.*, 1998), in this paper, our simulation is based on a simple thermal diffusion model, assuming an excitation of the material with a Gaussian pulse shape. As the pulse duration is much shorter than a time step in the simulation, the energy absorption with a laser pulse is assumed instantaneous. In our simulation, the input pulse energy is set as 200 nJ, and the corresponding absorptivity α_g used in this model is 30%, which fits to the results presented in (Miyamoto, Cvecek and Schmidt, 2011). The heat transfer and the corresponding temperature distribution is calculated with an explicit finite difference model. As shown in Fig 2-(a), three main mechanisms have be considered in the heat transfer processes: heat conduction, heat convection and thermal radiation.

Fig 2-(b) presents the temperature of the glass versus the exposure under different repetition rates. The probe point for the temperature evolution evaluation is set at a zenith position of 2 µm from the geometrical focal point. From the evolution curve one can see that, the heat accumulation effect is more efficient in the burst mode (with 8 pulses in a burst, and 20-ns pulse-to-pulse interval) compare to the normal mode with repetition rate of 500 kHz. Fig 2-(c) shows the temperature distribution near the focus after the exposure of the 8th pulses under two repetition conditions, the yellow dash line indicates the melting front of the glass. The direct comparison shows that, with the same number of pulses, in the burst mode, the glass temperature at the focus can be elevate to a higher value. In another words, to reach the same temperature, the burst mode requires less total energy, and as pointed out by Zimmermann (Zimmermann *et al.*, 2013), this could help to reduce the stress in the surroundings of the laser induced weld seams. Therefore, in the rest of this paper, we choose to use the burst mode, i.e. 125 kHz, 8 pulses per burst, for the welding experiments.

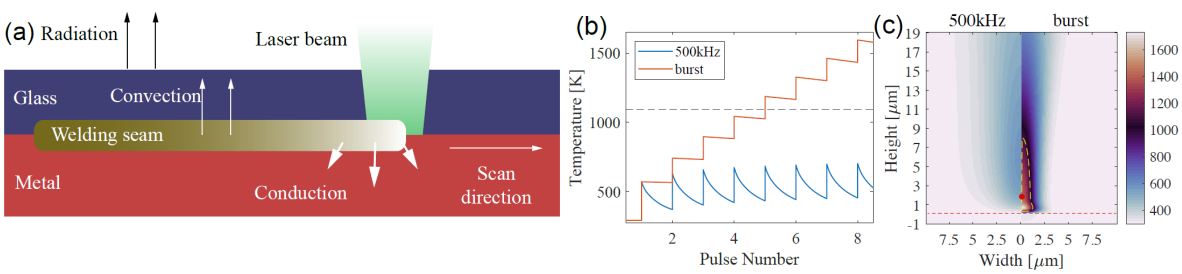

Fig. 2. (a) Principal mechanisms of the heat transfer in solid. (b) The temperature of the glass versus exposure, at a zenith position of 2-µm from the geometrical focal point. The dash line indicates the soft point of the Borofloat 33 glass. (c) The temperature distribution near the focus after the exposure of the 8th pulses. The left half represents the 500~kHz condition and the right half represents the burst (125 kHz, 8 pulses in a burst, pulse interval 20~ns) condition. The yellow dash line indicates the melting front, the red dash line is the glass-to-copper interface, and the red dot is the probe point for temperature evolution evaluation.

2.3. LIDT evaluation of the samples

To distinguish the processing windows in which the laser ablation of the metal or the laser-induced glass melting is predominate, and to anchor the parameters study, ahead of the welding, we performed the laser-induced damage threshold (LIDT) measurements at the front surface of the copper and the back surface of the Borofloat 33 glass (B33). The damage probability curves of each sample are presented in Fig 3, and the LIDT for the 0% damage probability of Borofloat33 is measured as 0.99 J/cm^2 and copper as 0.25 J/cm^2.

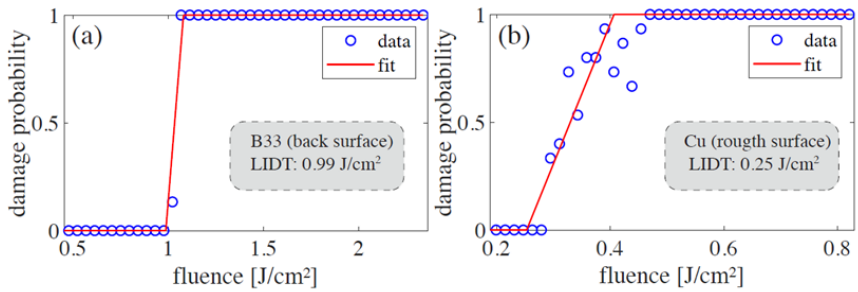

Fig. 3. Laser-induced damage threshold (LIDT) probability curve of (a) Borofloat 33 glass, and (b) copper.

3. Welding results

3.1. Effect of the pulse energy on the weldability

As we have mentioned in the introduction, according to the currently available literature, there are two contradictory interpretations on the USP laser glass-to-metal welding. The first one believes that the adhesives are attribute to the ablation-induced metal particles, and the maximum bridgeable gap size depends on the stacking height of the ablated particles. The second interpretation believe that the glass melting and having the molten glasses fill the gap is instrumental in metal-glass welding.

To figure out which interpretation is closer to the nature of the successful welding, we need to first find the processing regime in which the laser ablation of the metal is predominate and there is not laser-induced melting of the glass. Besides, to achieve the comparable results, the focal position is set as 20 µm below the glass-copper interface. Under this focal condition, the LIDTs are measured at the front surface of the copper and the back surface of B33 samples. Using the LIDT values as the anchors, three different regions in terms of input pulse energy are defined: (1) below copper LIDT, (2) higher than copper LIDT but lower than B33 LIDT and (3) higher than B33 LIDT. With the same scan speed (1mm/s) and line interval (20 µm); the welding experiments are performed under each region.

Fig 4 (a-c) show the SEM characterizations of the welding seams after the separation under different input pulse energies. In Fig 4 (a), the input pulse energy is 275% of the Cu LIDT and 68% of the B33 LIDT. Under this condition, the input pulse energy is high enough to create significant ablation on the Cu surface; however, it is not sufficient to lead the melting of the glass. From the SEM image, one can clearly see the ablation tracks on the copper surface with ablated particles stacking besides. According to the theory proposed by Zhang (Zhang and Cheng, 2015) and Matsuyoshi (Matsuyoshi *et al.*, 2018), the stacking of the micro/nanometer-size metal particles/debris produced by laser ablation of the metal will attach to the glass substrate and can act as the adhesive of the welding. However, the breaking strength corresponds to this case is 0.19 MPa in our experiments. This weak strength indicates that, by the ablated metal particles itself, it cannot achieve welding with the acceptable quality. According to the breaking strength tests presented in Fig 4 (d), it starts to achieve

significant bonding when the input pulse energy exceeds the glass LIDT. Fig 4 (b) presents the SEM analysis of the welding seam left on the copper surface after the breaking test, in which the input pulse energy is 0.66 µJ (275% of the glass LIDT). From the SEM image, one can clearly see that, residual glass blocks stand exactly upon the scanning tracks. Those resolidified glass directly proved that under this processing condition, there are molten glasses wetting the copper surface and forming the real contacts between the previously separated samples. The average breaking strength measured under this input pulse energy is 4 MPa. It is worth noting that, without further optimization (varying focus position, pulse energy, etc.), this value is already two times of the highest breaking strength reported by previous studies in which the ablated metal particles/debris was act as the adhesives.

Finally, as presented in Fig 4 (c), when the input pulse energy is too high (1.16 µJ, 480% of the glass LIDT), even though the molten glass can still wet the copper surface, the laser-induced explosive high pressure leads the complete separation of the molten glass and the glass substrate. Under this condition, the breaking strength decreased to 0.84 Mpa.

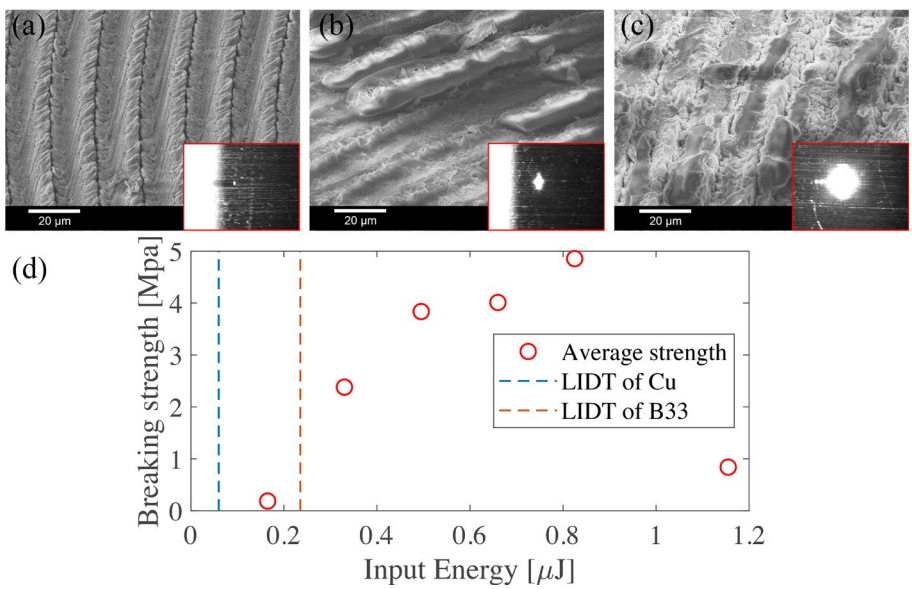

Fig. 4. SEM images of copper surface after the separation of the welded samples under different pulse energies (a) 68% of the glass LIDT (0.24 µJ), (b) 275% of the glass LIDT and (c) 480% of the glass LIDT. The insert sub-figures are the reflective microscopy snapshots recorded during the welding process. (d) The average breaking strength of the welded sample under different input pulse energies. The dash lines indicate the LIDT of Cu (0.06 µJ) and B33 (0.24 µJ) when the laser is focused at 20 µm below the interface.

From the three typical processing conditions (Fig 4 (a-c)), we have discovered that, the successful welding establishes when a continuous structure forms through the glass-weld-copper interfaces. To weld glass onto the copper with a rough surface, with the ablated metal particles itself, electronically continuous structures are unlikely to form. Even the stacking of the ablated particles can bridge the gap and form junctions between the substrates, given the nature that the debris-to-debris and the debris-to-substrate adhesion force is dominated by the LW interaction (Glover, 2003; Scholz and Dickmann, 2010), adhesion established through the debris is doomed weak. Continuous structures are more likely to form through the liquid glass emission; the copper surface is first wet by the liquid glass and form a localized intimate contact area, then within this area, the USP laser-induced micro plasma ensured the formation of the copper oxide layer.

In order to achieve this condition, it is necessary to have a stable ejection process to transfer the liquid form of one substrate material through the gap to another substrate. Within this transfer process, the splashing of the liquid would form debris/particles instead of continuous block. Given the nature that the debris-to-debris and the debris-to-substrate adhesion force is dominated by the LW interaction (Glover, 2003; Scholz and Dickmann, 2010), adhesion established through the debris is doomed weak. In the glass-to-copper welding condition, due to the glass-on-top layout and the high viscosity nature of the molten glass, it is more likely to have a stable liquid transfer without splashing through glass melting (with an intermediate input energy) (Dinca *et al.*, 2012).

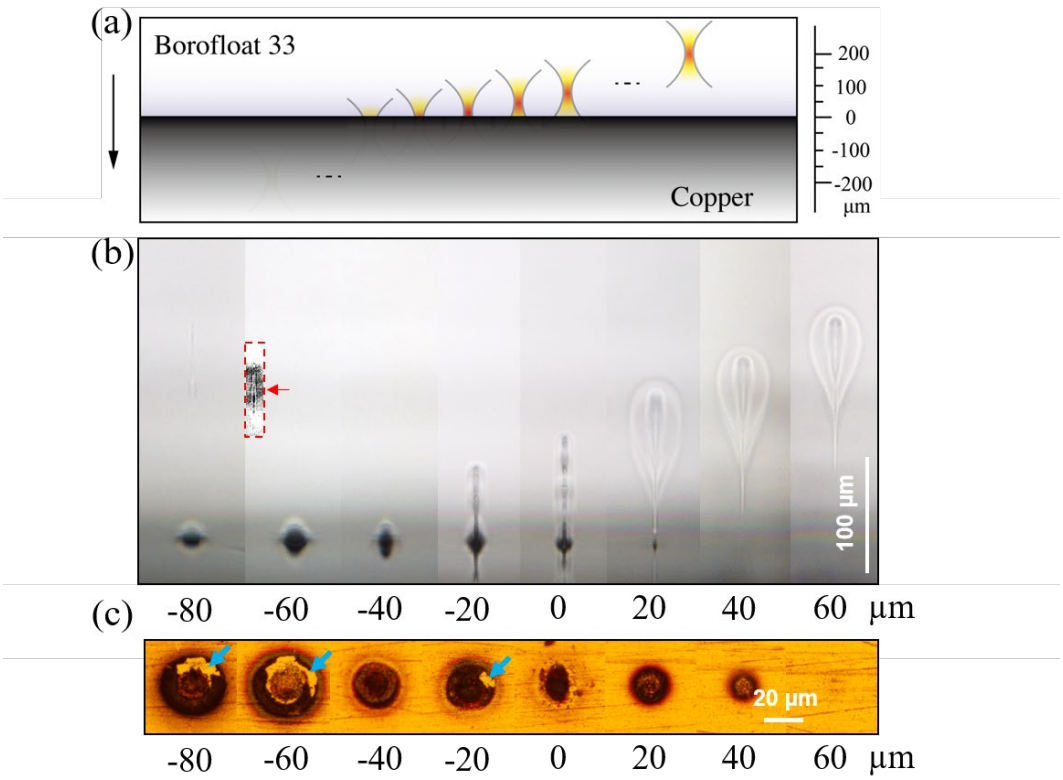

Fig. 5. (a) Notation of the focal position. Modifications under different focal positions in (b) glass and on (c) copper surface. The pulse energy is 0.8 µJ and the number of bursts per site is 1000. The blue arrows point on the footprints of the molten glass.

3.2. Effect of the focus position on the weldability

Another parameter that has strong influence to the successful welding is the focus position. In the glass-to-glass welding, the favorable focal position is in the range of 6-60 times of the Rayleigh length below the interface (Richter *et al.*, 2015). In such conditions, the molten material from the lower glass substrate will eject and deposit at the back surface of the upper substrate as soon as the upper tip of the modification reaches to the surface. In the glass-to-metal welding condition, according to our investigations in Section 3.1, to achieve successful welding, the molten material should come from the upper glass. In this section, we investigate the favorable focus position for the molten material ejection from the upper glass substrate and eventually its influence on the bonding strength.

Firstly, as shown in Fig 5, we investigate the single site modification at different focal position. As indicated by Fig 5 (a), for the notation, the focal position is note as 0 µm when the maximum intensity plane is located at the interface. Refers to that, the position is note as positive towards the glass direction and negative towards the metal direction. The pulse energy is kept as 0.8 µJ and the number of bursts per site is 1000. Based on a home-made software (Li *et al.*, 2021), by taking the planar interface induced aberration into account, the $1/e^2$ radius of laser beam is calculated as 1.86 µm at the focus and the Rayleigh length is calculated as 42 µm. As shown in Fig 5 (b-c), when the focal position is higher than 60 µm, modification only exist in the glass and it forms a teardrop-shaped inner structure, which corresponds to the electronically damaged zone, and an elliptical outer structure, which corresponds to the molten region. When the focal position is 20 or 40 µm above the interface, the modification structures can still preserve, however, the transmitted laser fluences are high enough to ablate the copper surfaces. When the focal position is located at the interface or 20 µm below the interface, the geometrical feature of the modifications is different. The increased voids along the inner structure and the decreased volume of the molten region indicates the emission of the molten materials. Besides, under those focal conditions, on the copper surface we can also detect the footprint of the molten glasses blocks upon the copper surface (pointed out by the blue arrows), which also indicates the emission of the molten glasses. When the focal position is lower than -60 µm, the back reflection induced modification starts to appear in the bulk of the glass (pointed out by a red arrow).

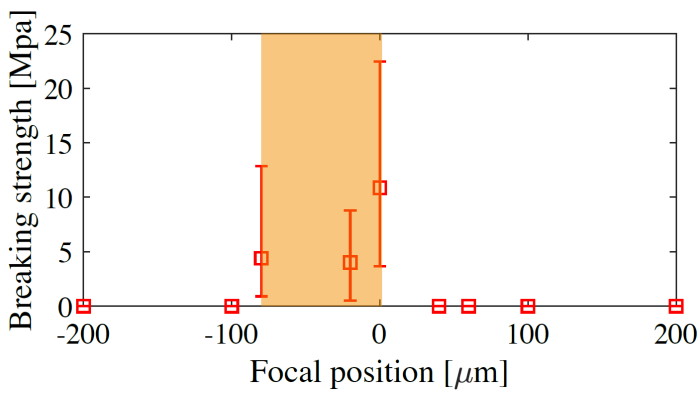

Fig. 6. The maximum breaking strength that can be achieved under different focal positions.

Finally, we performed glass-to-copper welding under different focal conditions. The translation speed of the sample is 1 mm/s. As expected, when the focal position is 40 µm above the interface, by metal ablation itself, no significant bonding has achieved no matter how the input pulse energy adjusted. On the other hand, when the focal position more than 100 µm below the interface it is also difficult to form significant bonding due to the back reflection. In Fig 6, we used the orange color to mark out the process windows of the successfully welding in terms of the focal position. To make to results obtained at different focal position comparable, for each position, we first perform an energy scan to find the optimized processing energy; afterwards, with this optimized energy, we repeat the welding experiments by five times and calculated the average breaking strength of the welds. The maximum value of this average breaking strength is 10.9 Mpa, and it is obtained when the foal position is overlapped with the interface. However, it is worth noting that, due to the surface roughness and the lack of clamping assistance, the deviation of the breaking strength is large. This feature might be a problem for the standardized production; however, this does not detract its value in the assembling application where external clamping is prohibited.

4. Discussions and conclusions

In this paper, we investigate the glass to surface-unpolished metal welding without the any assistance of the clamping system. According to the previous researches, there are two contradictory interpretations on the USP laser glass-to-metal welding without optical contact. The first one believes that the adhesives are attribute to the ablation-induced metal particles, and the maximum bridgeable gap size depends on the stacking height of the ablated particles. The second interpretation believe that the glass melting and having the molten glasses fill the gap is instrumental in metal-glass welding. Our experimental investigations presented in this paper support the second interpretation. Furthermore, we have discovered the processing windows in terms of pulse energy and focal position for our specific surface condition (Ra 272 nm and Rz 1.89 µm). Finally, without clamping, the maximum average breaking strength of the B33-to-copper weld is measured as 10.9 Mpa.

Acknowledgements

This research has been supported by the Bundesministerium für Bildung und Forschung (BMBF) through the glass2met project, grant no. 13N15290.

References

Carter, R. M. *et al.* (2014) 'Picosecond laser welding of similar and dissimilar materials', *Applied Optics*, 53(19), p. 4233. doi: 10.1364/ao.53.004233.
Carter, R. M. *et al.* (2017) 'Towards industrial ultrafast laser microwelding: SiO_2 and BK7 to aluminum alloy', *Applied Optics*, 56(16), p. 4873. doi: 10.1364/AO.56.004873.
Chambonneau, M. *et al.* (2021) 'Taming Ultrafast Laser Filaments for Optimized Semiconductor–Metal Welding', *Laser and Photonics Reviews*. Wiley-VCH Verlag, 15(2), p. 2000433. doi: 10.1002/lpor.202000433.
Chen, H. *et al.* (2019) 'Picosecond laser welding of glasses with a large gap by a rapid oscillating scan', *Optics Letters*, 44(10), p. 2570. doi: 10.1364/ol.44.002570.
Chen, J. *et al.* (2015) 'Avoiding the requirement for pre-existing optical contact during picosecond laser glass-to-glass welding', *Optics Express*. Optical Society of America, 23(14), p. 18645. doi: 10.1364/oe.23.018645.
Ciuca, O. P. *et al.* (2016) 'Characterisation of weld zone reactions in dissimilar glass-to-aluminium pulsed picosecond laser welds', *Materials Characterization*, 120, pp. 53–62. doi: 10.1016/j.matchar.2016.08.013.
Cvecek, K. *et al.* (2015) 'Gap bridging in joining of glass using ultra short laser pulses', *Optics Express*, 23(5), p. 5681. doi: 10.1364/OE.23.005681.
Dinca, V. *et al.* (2012) 'Influence of solution properties in the laser forward transfer of liquids', in *Applied Surface Science*. Elsevier B.V., pp. 9379–9384. doi: 10.1016/j.apsusc.2012.02.007.
Glover, T. E. (2003) 'Hydrodynamics of particle formation following femtosecond laser ablation', *Journal of the Optical Society of America B*. The Optical Society, 20(1), p. 125. doi: 10.1364/josab.20.000125.
Kanavin, A. P. *et al.* (1998) *Heat transport in metals irradiated by ultrashort laser pulses*.
Li, Q. *et al.* (2021) 'Flexible, fast, and benchmarked vectorial model for focused laser beams', *Applied Optics*. The Optical Society, 60(13), p. 3954. doi: 10.1364/AO.421945.
Matsuyoshi, S. *et al.* (2018) 'Welding of Glass and Copper with a Rough Surface using Femtosecond Fiber Laser Pulses', *JLMN-Journal of Laser Micro/Nanoengineering*, 13(1). doi: 10.2961/jlmn.2018.01.0005.
Miyamoto, I. *et al.* (2015) 'High speed, high strength microwelding of Si/glass using ps-laser pulses', *Optics Express*, 23(3), p. 3427. doi: 10.1364/OE.23.003427.
Miyamoto, I., Cvecek, K. and Schmidt, M. (2011) 'Evaluation of nonlinear absorptivity in internal modification of bulk glass by ultrashort laser pulses', *Optics Express*, 19(11), p. 10714. doi: 10.1364/OE.19.010714.
Penilla, E. H. *et al.* (2019) 'Ultrafast laser welding of ceramics', *Science*, 365(6455), pp. 803–808. doi: 10.1126/science.aaw6699.
Richter, S. *et al.* (2013) 'Ultrashort high repetition rate exposure of dielectric materials: laser bonding of glasses analyzed by micro-Raman spectroscopy', *Applied Physics A*, 110(1), pp. 9–15. doi: 10.1007/s00339-012-7478-1.

Richter, S. *et al.* (2015) 'Toward laser welding of glasses without optical contacting', *Applied Physics A*, 121(1), pp. 1–9. doi: 10.1007/s00339-015-9377-8.
Scholz, T. and Dickmann, K. (2010) 'Investigation on particle formation during laser ablation process with high brilliant radiation', in *Physics Procedia*. Elsevier B.V., pp. 311–316. doi: 10.1016/j.phpro.2010.08.151.
Zhang, G. *et al.* (2017) 'Interface modification based ultrashort laser microwelding between SiC and fused silica', *Optics Express*. The Optical Society, 25(3), p. 1702. doi: 10.1364/oe.25.001702.
Zhang, G. and Cheng, G. (2015) 'Direct welding of glass and metal by 1 kHz femtosecond laser pulses', *Applied Optics*, 54(30), p. 8957. doi: 10.1364/AO.54.008957.
Zimmermann, F. *et al.* (2013) 'Ultrastable bonding of glass with femtosecond laser bursts', *Applied Optics*, 52(6), pp. 1149–1154. doi: 10.1364/AO.52.001149.